Available online at www.sciencedirect.com
ScienceDirect
Ceramics International 35 (2009) 463–466
CERAMICS INTERNATIONAL
www.elsevier.com/locate/ceramint

Development of metal oxide nanoparticles by soft chemical method

M.I.B. Bernardi [a,*], C.A.C. Feitosa [b], C.A. Paskocimas [c], E. Longo [d], C.O. Paiva-Santos [d]

[a] Grupo de Crescimento de Cristais e Materiais Cerâmicos, Instituto de Física de São Carlos, USP, São Carlos, Av. Trabalhadores São-carlense 400, P.O. Box 369, 13560-970 São Carlos, SP, Brazil
[b] Departamento de Física, Centro Tecnológico da Universidade Federal do Maranhão, Campus do Bacanga, 65085-580 São Luis, MA, Brazil
[c] Departamento de Engenharia Mecânica, Universidade Federal do Rio Grande do Norte, Campus Lagoa Nova, 59072-970 Natal, RN, Brazil
[d] Centro Multidisciplinar de Desenvolvimento de Materiais Cerâmicos, CMDMC, Instituto de Química, UNESP, 14800-900 Araraquara, SP, Brazil

Received 16 October 2007; received in revised form 6 November 2007; accepted 2 January 2008
Available online 8 April 2008

Abstract

An extensive work for the study of SnO_2 samples doped with x-mol% of Sb (x = 0, 6, 10, 14 and 18) is reported. The materials were prepared by the polymeric precursor method (Pechini method), calcined for 4 h between 800 °C and 1200 °C. The Rietveld method with X-ray diffraction data (XRD) was used to analyze the unit cell dimensions, crystallite size and microstrain. It was observed the crystallite size increasing and decrease of the microstrain with the increase of the calcining temperature. The synthesis of tin oxide nanoparticles with high thermal stability against particle growth rate was achieved by doping SnO_2 particles with Sb_2O_3. All the phases tend to have the same dimension when the temperature increases, although its values varies with x and reaches the maximum value when fired at 1100 °C. These variations seem to be an indication that the oxidation state of the antimony changes with the amount of Sb added to the material.

Keywords: A. Powders: chemical preparation; B. Electron microscopy; B. X-ray methods; SnO_2:Sb; Pigments

1. Introduction

Tin dioxide is a ceramic material with many interesting applications, for example catalysts, gas sensors, optoelectronic or photovoltaic devices [1–5], that requires specific characteristics like films, dense or porous materials for technological use and are directly related to the particles size.

It is known that the traditional source of blue color in currently known ceramic pigments contains Co [6]. In this work is presented an alternative to these systems with the antimony incorporation in the host lattice of SnO_2, which can decrease the environmental impact in the manufacturing process (Co is widely considered as toxic or hazardous), while also maintain an optical coloring performance in the desired glaze. The coloring performance of pigments depends very much on its thermal stability, chemical reactivity towards the glaze components, the coordination of host ions, and it was also noticed a great dependence on the methodology used to prepare it [7].

In this work were studied the Sb dopant and calcining temperature influences on the microstructure (size-strain), unit cell parameters and particles size of SnO_2 prepared by soft chemical route well known as Pechini method. The weighted size-strain method, described elsewhere [8], was applied for the microstructural analysis. The high resolution transmission electron microscopy (HRTEM) was used to observe the morphologic aspects and measure the size of the particles.

2. Experimental

SnO_2 samples doped with x-mol% of Sb (x = 0, 6, 10, 14 and 18) were prepared through Pechini method [9,10]. The process is based on metallic citrate polymerization using ethylene glycol. Citric acid was used to chelate cations in an aqueous solution. The addition of ethylene glycol leads to the formation of an organic ester. Polymerization, promoted by heating the mixture, results in a homogeneous resin in which metal ions are uniformly distributed throughout the organic matrix. Details of the sample preparation are described elsewhere [11].

* Corresponding author. Tel.: +55 16 33739828; fax: +55 16 33739824.
E-mail address: m.basso@if.sc.usp.br (M.I.B. Bernardi).

0272-8842/$34.00
doi:10.1016/j.ceramint.2008.01.001

The treatment temperature ranged from 800 °C to 1200 °C, and the resulting powders were characterized by the Rietveld method with X-ray diffraction data. The XRD measurements were performed in a D5000 Siemens diffractometer, from 20 to 110° 2θ with $\Delta 2\theta = 0.02°$ 2θ, divergence slit = 2 mm, receiving slit = 0.6 mm, step time = 10 s, and copper radiation monochromatized by graphite crystal. The instrumental broadening was measured from a SiO_2 standard sample crashed from a single crystal. It was used a modified version the Rietveld refinement program DBWS 9807c [8], which is an upgraded version of the DBWS 9411 program [12].

In all samples it was observed only the SnO_2 phase. The initial FWHM parameters were that of the α-SiO_2 standard sample. At the beginning, it was refined the scale factor, sample displacement, cell parameters and background. After that, the FWHM parameters *U*, *Z*, *X* and *Y* were released to refine and then fixed again. Then the individual atom displacements parameters and the oxygen positional parameters were refined. It was observed small peaks at the low angle side of all SnO_2 peaks, which were caused by the L_α radiation of the tungsten. Then it was considered another SnO_2 phase with unit cell 4.48% greater than the first one, to fit that peaks caused by the W_{L_α} radiation. The refinement was considered complete when all parameters shifts were less than 10% of the standard deviations.

The HRTEM was used to observe the morphologic aspects of the particles and to measure its sizes.

3. Results and discussion

Fig. 1 shows the Rietveld plot for the sample calcined at 1000 °C/4 h for $x = 0.14$, where it is possible to observe the good agreement between the observed and calculated pattern. It is also shown there the Bragg peaks of the second supposed SnO_2 phase used to fit the tungsten L_α radiation.

The final unit cell parameters are in Table 1, the unit cell volume variation can be observed in Fig. 2; the crystallite size and microstrain are in Fig. 3.

The final Rietveld refinement indexes, defined by Young and Wiles (1982) [13] had been the maximum value of 1.42 of the goodness of fit index (*S*) indicates that the profile agreement was of good quality for all samples. The Bragg intensity index

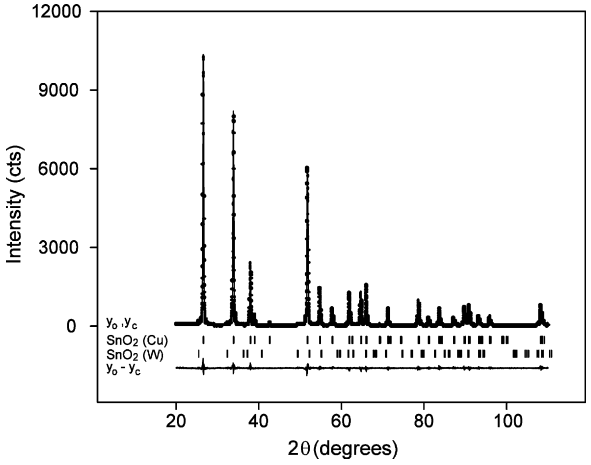

Fig. 1. Rietveld plot for the sample calcined at 1000 °C/4 h for $x = 0.14$.

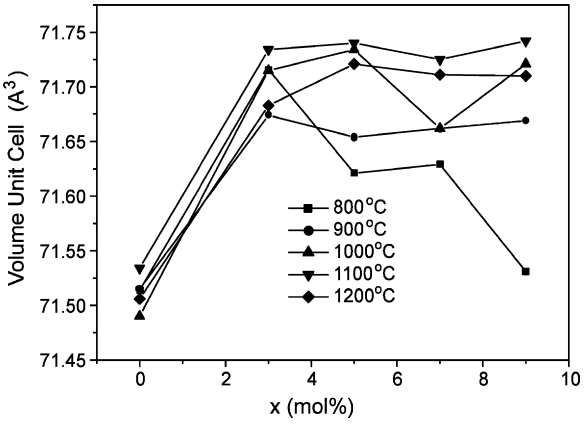

Fig. 2. Unit cell volume variation in function of the Sb_2O_3 concentration.

(R_B) for all refinements are very low, indicating that the crystal structure model refined is in good agreement with the observed data.

One can note in Figs. 2 and 3:

(a) The unit cell is larger for the doped materials.
(b) The largest unit cell is reached for the material heated at 1100 °C.

Table 1
Unit cell parameters of the SnO_2 for the different systems

	Unit cell (Å)	800 °C	900 °C	1000 °C	1100 °C	1200 °C
$x = 0$	*a* (Å)	4.73742(8)	4.73745(7)	4.73690(5)	4.73791(6)	4.73718(4)
	c (Å)	3.18648(6)	3.18648(5)	3.18610(4)	3.18670(5)	3.18644(3)
$x = 3$	*a* (Å)	4.74118(2)	4.74036(1)	4.74101(5)	4.74138(4)	4.74037(4)
	c (Å)	3.19038(1)	3.18962(1)	3.19057(4)	3.19089(3)	3.19000(3)
$x = 5$	*a* (Å)	4.73926(2)	4.73989(1)	4.74134(5)	4.74149(4)	4.74111(4)
	c (Å)	3.18873(2)	3.18937(9)	3.19097(4)	3.19105(3)	3.19068(3)
$x = 7$	*a* (Å)	4.73907(2)	4.73989(1)	4.74120(5)	4.74160(4)	4.74098(4)
	c (Å)	3.18934(2)	3.18978(7)	3.19077(4)	3.19107(3)	3.19046(3)
$x = 9$	*a* (Å)	4.73755(2)	4.74021(1)	4.74118(5)	4.74155(5)	4.74090(4)
	c (Å)	3.18701(2)	3.18963(7)	3.19062(4)	3.19102(4)	3.19049(3)

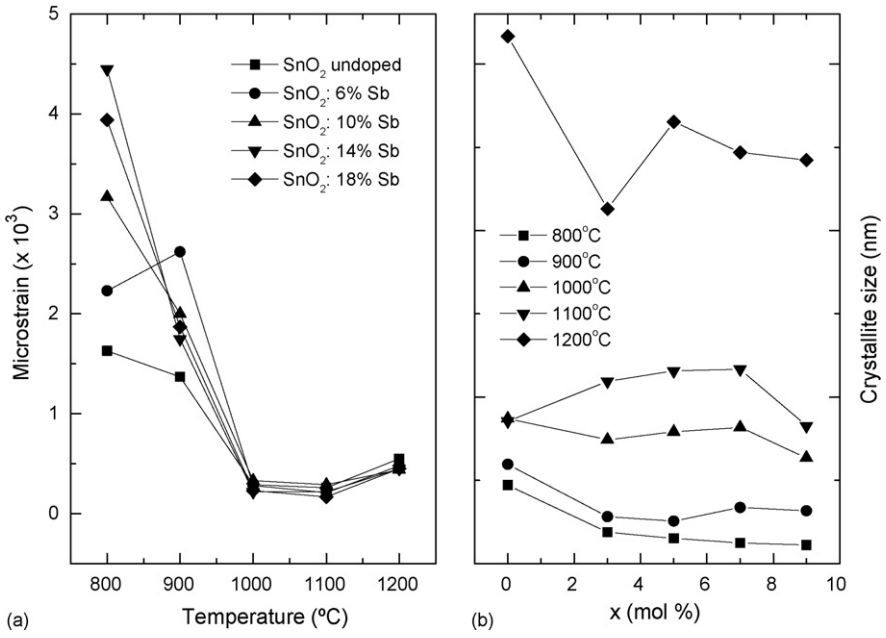

Fig. 3. (a) Crystallite size variation in function of the Sb_2O_3 concentration and (b) microstrain variation in function of the heating temperature.

(c) The unit cell for the doped materials is almost constant for each temperature of treatment, excepted when calcined at 800 °C.
(d) Microstrains are the same for all samples at 1000 °C and 1100 °C; and for 1200 °C they are shortly larger.
(e) Microstrain decrease with the temperature to a minimum value around 0.02%.
(f) The crystallite size increases with the heating temperature, and they are the greatest for the undoped sample.

The microstructure of a material is sensibly altered by the dopants addition, mainly, when the substitute atom has characteristics, as the valence, very different from the presented by the central atom to be substituted.

The amount of dopants tends to influence the mechanism of growth of the SnO_2 particles. The addition of 10% atomic ratio of vanadium to the tin dioxide, synthesized by co-precipitation, causes the decrease of the crystallite size average and the increase of the microstrain of the material [14]. SnO_2 doped with manganese (0.3, 0.5, 0.7 and 1 mol%), obtained by Pechini method, presented considerable decrease in the crystallite size with the increase of the concentration of manganese and segregation in the grain boundary for the samples synthesized in higher temperatures [15]. Leite et al. observed a decrease of

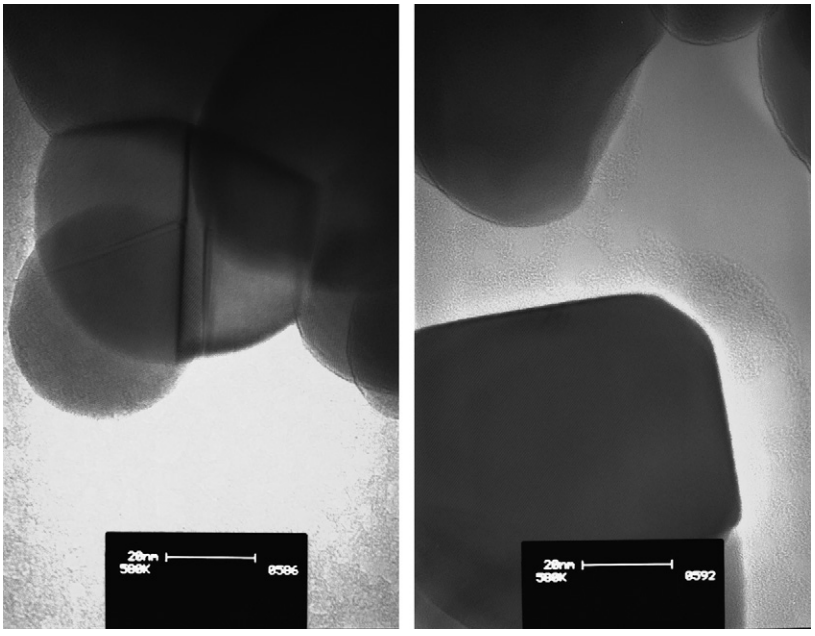

Fig. 4. HRTEM images of SnO_2:7Sb (mol%) (left) and undoped SnO_2 (right). Both powders were heated using the same time and temperature.

the crystallite size average and a considerable increase of the surface area in 5 mol% of Nb_2O_5 doped SnO_2, compared with the pure one [16].

In this work was also observed the decrease of the crystallite size average and a considerable increase of the surface area, when compared with pure SnO_2. In a previous work, Leite et al. [17] did not observe phase segregation in these materials by XPS (X-ray photoelectron spectroscopy). The XRD measurements also did not show an evidence of a second phase in the range of temperature studied.

During the heating, the antimony can be present with the two oxidation state (3+ and 5+) with different ionic radii. For coordination number 6, the ionic radii is 0.069 nm for Sn^{4+}, 0.060 nm for Sb^{5+} and 0.076 nm for Sb^{3+}[18]. Kojima et al. [19] observed that at low amounts of Sb ions the predominant oxidation state is 5+. For heavily-doped SnO_2, it is suggested that some of the Sn^{4+} ions in the SnO_2 lattice are replaced by Sb^{3+} ions.

In fact, that is also observed by the increase of the unit cell parameters (a, b, V) with the increase of the antimony addition in the SnO_2 lattice. The entrance of Sb^{3+} in the lattice can create oxygen vacancies, originating cations repulsion and a unit cell increasing. The increase of the unit cell is also consequence of the largest ionic radii of Sb^{3+} when compared to the Sn^{4+}.

For higher concentrations of Sb, oxidation of Sb^{3+} to Sb^{5+} occurring at 800 °C favors the incorporation of Sb into the SnO_2 lattice, because of the lower ionic radius of Sb^{5+} (as compared of Sb^{3+}). This fact accounts for the unit cell shrinkage finally observed. Temperatures above 900 °C until 1100 °C are enough to allow the entrance of larger amount of antimony, providing the coexistence of ions with both oxidation 3+ and 5+. This maintains constant the number of vacancies, the unit cell, the microstrain and the crystallite size. For the material heated at 1200 °C, a decrease of the Sb^{3+} species in relation to species Sb^{5+} occurs, causing an increasing of the crystallite size, microstrain and shortly reducing of the unit cell.

Fig. 4 show the HRTEM images of SnO_2:7% Sb_2O_3 (mol%) and undoped SnO_2. It can be observed that the doped SnO_2 is arranged into individual particles with a few coalescence particles. Well-defined necks between particles are observed in the case of undoped SnO_2 particles, indicating an advanced stage of particle coalescence. The HRTEM analysis showed that the undoped material is more densely agglomerated than the doped material. These results clearly show that doped Sb can be used to control particle size and stabilize SnO_2 against particle growth at high temperatures.

4. Conclusions

The increase of the unit cell is due to the substitution of Sn^{4+} by Sb^{3+} in the SnO_2 lattice. Sb^{3+} and Sb^{5+} coexist at higher concentration of antimony for the materials heated above 900 °C, causing the stability of crystallite size and microstrain. For the material prepared at 800 °C, the amount of Sb^{5+} increase with the addition of antimony. The HRTEM analysis showed that the undoped material is more densely agglomerated than the doped material. These results clearly show that doped antimony can be used to control particle size and stabilize SnO_2 against particle growth at high temperatures.

Acknowledgements

The authors gratefully acknowledge the financial support of the Brazilian financing agencies FAPESP, CNPq/PRONEX and CAPES.

References

[1] Z.M. Jarzebski, J.P. Marton, J. Electrochem. Soc. 129 (1976) 299C–310C.
[2] J.G. Fagan, V.R.W. Amarakoon, Am. Ceram. Bull. 72/73 (1993) 119–129.
[3] M.H. Islam, C.A. Hogarth, J. Mater. Sci. Lett. 8 (1989) 989–992.
[4] W. Göpel, K.D. Shierbaum, Sens. Actuators B 26/27 (1995) 1–12.
[5] E. Traversa, J. Am. Ceram. Soc. 78 (1995) 2625–2632.
[6] R.K. Mason, Am. Ceram. Soc. Bull. 40 (1) (1961) 5–6.
[7] J.J. Gomés, J.B. Carda, A. Nebot, J.V. Canceler, M.A. Jovani, A. Soler, Cerámica Información 250 (1999) 1–24.
[8] C.O. Paiva-Santos, H. Gouveia, W.C. Las, J.A. Varela, Mater. Struct. 6 (2) (1999) 111–114.
[9] C.O. Paiva-Santos, A.A. Cavalheiro, M.A. Zaghete, M. Cilense, J.A. Varela, M.T.S. Giotto, Y.P. Mascarenhas, Adv. X-ray Anal. 44 (2001) 38–43.
[10] M. Pechini, Method of Preparing Lead and Alkaline-Earth Titanates and Niobates and Coating Method Using the Same to Form a Capacitor, US Pat. 3,330,697 (1967).
[11] I.T. Weber, E. Longo, E.R. Leite, Mater. Lett. 43 (2000) 166–169.
[12] M.I.B. Bernardi, L.E. Soledade, I.A. Santos, E.R. Leite, E. Longo, J.A. Varela, Thin Solid Films 405 (2002) 228–233.
[13] R. Young, A. Sakthivel, T.S. Moss, C.O. Paiva-Santos, J. Appl. Cryst. 28 (1995) 366–367.
[14] L. Sangaletti, L.E. Depero, B. Allieri, F. Pioselli, R. Angelucci, A. Poggi, A. Tagliani, S. Nicoletti, J. Eur. Ceram. Soc. 19 (1999) 2073–2077.
[15] Y. Shimizu, S. Kai, Y. Takao, T. Hyodo, M. Egashira, Sens. Actuators B 65 (2000) 349–357.
[16] E.R. Leite, I.T. Weber, E. Longo, J.A. Varela, Adv. Mater. 12 (2000) 965–968.
[17] E.R. Leite, M.I.B. Bernardi, E. Longo, J.A. Varela, C.A. Paskocimas, Thin Solid Films 449 (2004) 67–72.
[18] R.D. Shannon, Acta Crystallogr. A32 (1976) 751–767.
[19] M. Kojima, H. Kato, M. Gatto, Philos. Mag. B 73 (1996) 277–288.